

University of Texas Rio Grande Valley

ScholarWorks @ UTRGV

Physics and Astronomy Faculty Publications
and Presentations

College of Sciences

2004

Generation of the Transient Electrical and Spontaneous Magnetic Fields by Solid State Combustion

Karen S. Martirosyan

The University of Texas Rio Grande Valley

J. R. Claycomb

J. H. Miller Jr.

D. Luss

Follow this and additional works at: https://scholarworks.utrgv.edu/pa_fac



Part of the [Astrophysics and Astronomy Commons](#), and the [Physics Commons](#)

Recommended Citation

Martirosyan, K. S., et al. "Generation of the Transient Electrical and Spontaneous Magnetic Fields by Solid State Combustion." *Journal of Applied Physics*, vol. 96, no. 8, American Institute of Physics, Oct. 2004, pp. 4632–36, doi:10.1063/1.1788845.

This Article is brought to you for free and open access by the College of Sciences at ScholarWorks @ UTRGV. It has been accepted for inclusion in Physics and Astronomy Faculty Publications and Presentations by an authorized administrator of ScholarWorks @ UTRGV. For more information, please contact justin.white@utrgv.edu, william.flores01@utrgv.edu.

Generation of the transient electrical and spontaneous magnetic fields by solid state combustion

K. S. Martirosyan

Department of Chemical Engineering University of Houston, Houston, Texas 77204

J. R. Claycomb

Department of Mathematics and Physics, Houston Baptist University, Houston, Texas 77074

J. H. Miller, Jr.

Department of Physics and Texas Center for Superconductivity and Advanced Materials, University of Houston, Houston, Texas 77204

D. Luss^{a)}

Department of Chemical Engineering, University of Houston, Houston, Texas 77204

(Received 3 May 2004; accepted 12 July 2004)

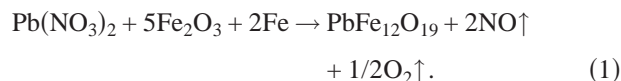
Experiments revealed that transient electric field intensities up to 2.5 V/cm were generated during the initial period of combustion synthesis of the ferromagnetic products before the maximum temperature was reached. This occurred when the iron particles were partially oxidized and the reaction product was mainly magnetite (Fe_3O_4). The electromagnetic field caused spontaneous magnetization of the product in the postcombustion zone. Magnetic field values up to 4 μT formed after the sample temperature fell below the Curie temperature and the initial reactants were completely converted to the ferromagnetic phase $\text{PbFe}_{12}\text{O}_{19}$. Increasing the volume of the samples increases the absolute residual magnetic field magnitude after cooling. We present possible mechanisms of the electromagnetic field generation during the combustion. © 2004 American Institute of Physics. [DOI: 10.1063/1.1788845]

I. INTRODUCTION

Solid state combustion synthesis is used to manufacture a wide variety of advanced multifunctional materials.^{1–3} Several experimental studies revealed that the high-temperature front motion during the combustion synthesis of ferromagnetic materials generated an electrical voltage and a residual magnetic field of about 1 V and 10 μT , respectively.^{4–8} A slowly oscillating field up to 20 nT was generated during the combustion in oxygen of various pure metals Ti, Zr, Mn, Nb, Fe, etc.⁹ Different modes of combustion front motion, i.e., spin, pulsating, and planar combustion synthesis of ferrites generated qualitatively different magnetic field spatial distribution. The average magnetization vector generated by either planar or pulsating combustion was oriented at a smaller angle with respect to the pellet axis ($\phi \leq 45^\circ$) than those generated by spin combustion ($60^\circ \leq \phi \leq 80^\circ$). The Earth's magnetic field had no impact on the spontaneous magnetization of the samples.¹⁰ At present, simultaneous measurements of the electrical field, spontaneous magnetization, combustion temperature, and conversion degree are not available. Also no established mechanism exists which explains the generation of the temporal electric fields and spontaneous magnetization during the combustion of either ferromagnetic or nonferromagnetic materials.

To enhance our understanding of these phenomena we studied the formation and temporal variation of electric and

magnetic fields, temperature and phase transformation during the combustion synthesis of hard magnetic materials, such as lead hexaferrite $\text{PbFe}_{12}\text{O}_{19}$,



These data enable us to determine the temperature at which the local electrical signal forms and decays, as well as the relation between the temporal voltage/current and the rate of temperature rise, magnetization, and conversion. We also report the relation between the residual magnetic field (RMF) of the cooled combustion products and the sample bulk capacity (diameter and length variation).

II. EXPERIMENT

All the reactants were 99+% pure (Sigma-Aldrich Chemical Company). The iron oxide and lead nitrate were dried at 115 °C for 5 h and then mixed with the metal powder for 1 h in a ball mill (US Stoneware, Mahwah, NY) before the combustion. Various cylindrical samples 12, 18, and 30 mm in diameter and 10, 20, and 30 mm long with initial porosity of about 50% were made by green charge pressing. Reaction (1) was conducted in air and was initiated by an electrically heated coil at the top of the sample. The electrical current to the coil was terminated immediately after the ignition to avoid electromagnetic perturbations during the measurements.

The combustion temperature, voltage, and magnetic fields were simultaneously measured in the experimental setup shown in Fig. 1. The temporal electric voltage was

^{a)}Electronic mail: Dluss@uh.edu

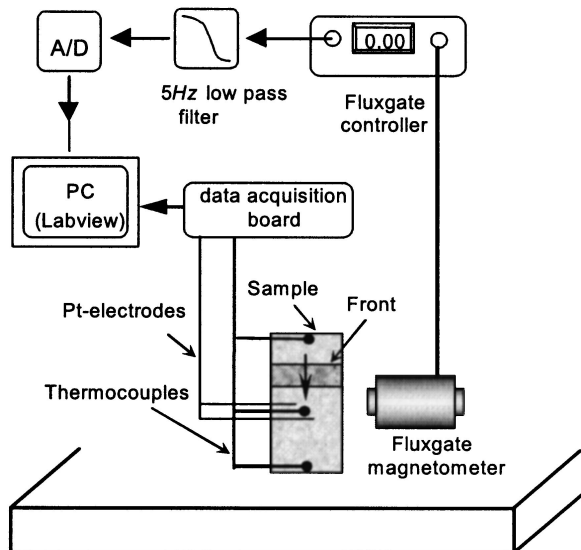


FIG. 1. Schematic of the experimental setup used for simultaneously measuring temporal temperature, intrinsic electrical signal, and spontaneous magnetization generated by combustion synthesis of ferrites.

measured between two Pt-electrodes ($\varnothing=0.1$ mm) separated by ~ 2 mm from each other and located in a cross section of the sample with one electrode connected to ground. The temperatures in the top, bottom, and middle of the sample were measured by three S-type (Pt-Rh) thermocouples (0.1 mm diameter) inserted close to the sample axis. The thermocouple in the middle of the sample was placed near the electrodes, so that the combustion front passed by the thermocouple and electrodes at the same time. The electrical signals were recorded by an Omega Data acquisition board connected to a PC. The impedance during the voltage and current measurements was 0.25 M Ω and 0.1 Ω , respectively. The temperature distribution of the sample was monitored by a high-speed IR digital video camera (Indigo Systems).

The spontaneous magnetic field was measured with an Applied Physics Systems fluxgate magnetometer located near the middle of the sample. The distance between the sensor and the sample was about 10 mm. The sensor was oriented normal to the sample axis, measuring the magnetic field horizontal component $B_h(t)$ (perpendicular to the direction of front propagation). The data were acquired with a Labview program after analog-digital conversion and 5 Hz low pass filtering.

The quenched front method³ was used to determine the phase transformation and product conversion degree during the combustion. These experiments were conducted in a massive copper cylinder 62 mm high with a conical hole 20 mm at the top and 1 mm at its bottom. The cylinder was made of two separable halves to enable characterization of the dependence of the chemical composition on position. Following ignition at the top, the front extinguishes before reaching the bottom of the cone. The quenching rate was estimated at 10^3 – 10^4 K/s.

The composition profile within the reaction zone was determined by X-ray diffraction (XRD) analysis (Siemens D5000; Cu K_α radiation source). The patterns were recorded in the range of $20^\circ \leq 2\theta \leq 70^\circ$ with $0.1^\circ \text{ min}^{-1}$ steps. The

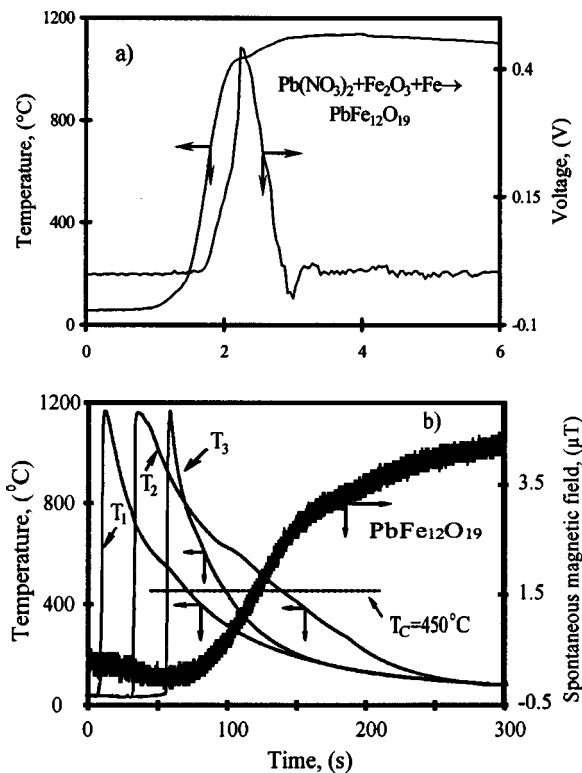


FIG. 2. (a) Temporal temperature and electric voltage generated by a combustion front during the combustion synthesis of lead hexaferrite. Distance between two electrodes 2 mm; (b) Three temporal combustion temperature of the sample in the top (T_1), middle (T_2), bottom (T_3) and spontaneous magnetic field near one side of the sample measured during solid combustion of lead ferrite, (T_C — Curie temperature). Distance between sample surface and sensor is 10 mm.

average combustion front velocity was determined from the time that the temperature wave moved through the sample.

III. RESULTS AND DISCUSSION

Figure 2(a) shows the temporal voltage and temperature generated by the combustion front. The electrical signal appeared when the temperature was ~ 520 °C. The maximum voltage and current of about 0.45 V and 15 mA were attained when the temperature was 1040 °C. The electrical voltage rise time was about 0.5 s and it decayed in ~ 0.9 s. The voltage vanished at a temperature of 1100 °C, before the maximum combustion temperature of 1150 °C was attained. The maximum electrical field intensity and current density was 2.5 V/cm and 5 A/cm², respectively.

The temporal combustion temperatures at the top, middle, and bottom of the sample (measured by thermocouples) and the corresponding magnetic field are shown in Fig. 2(b). The combustion front motion generated a slowly increasing magnetic field with a maximum value of about 4 μT . The spontaneous magnetic field started to form after the temperature at the ignition location decreased to about 450 °C, which is the Curie temperature of lead ferrite. The spontaneous magnetization rose slowly during the long cooling. The characteristic time of the spontaneous magnetization was about 250 s.

Figure 3 shows the dependence of the peak RMF of the cooled combustion products on the initial samples volume.

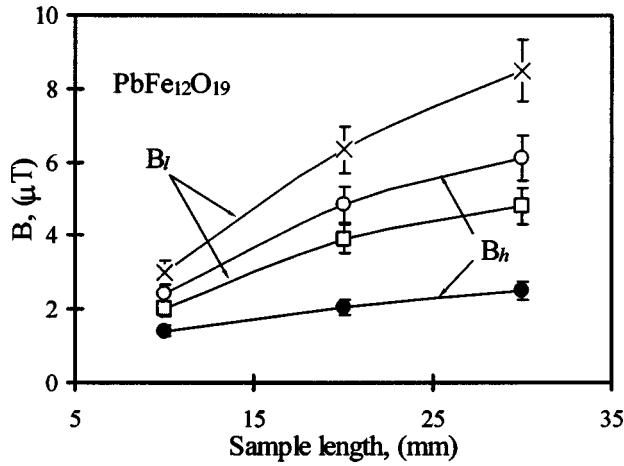


FIG. 3. Dependence of the peaks RMF of the cooled combustion products ($\text{PbFe}_{12}\text{O}_{19}$) on the initial sample length and diameter (\square , \bullet for $\varnothing = 12$ mm; \square , \times for $\varnothing = 30$ mm). B_l — longitudinal component of the magnetic field measured on top of a cylindrical samples; B_h — horizontal component measured on the side of a cylindrical surface surrounding the samples.

Note that for all samples the maximum RMF corresponded to the longitudinal component of magnetic field intensity B_l , was measured on top of the cylindrical samples with the south pole always at the ignition location. The horizontal field component B_h measured on the middle of the sample side was always less than longitudinal component of magnetic field intensity, $B_l > B_h$. This is consistent with the orientation of magnetic dipole moments along the main combustion axis with smaller radial field components depending on the combustion mode and the resulting anisotropies. The absolute value of the RMF increases almost linearly with increasing sample length while increasing the sample diameter 2.5 times increases the RMF less than twice. The RMF should be proportional to the square of the sample diameter (for uniform magnetization), which was not observed. This may be explained in part by a nonuniform current density through the porous media during the combustion. Also we expect transient magnetic fields to be larger, on average, closer to the cylindrical surface. Note that a uniform current density along the pellet axis would generate a magnetic field that is zero at the center, maximal at the surface that falls off with the square of the distance from the center, outside the pellet.

X-ray diffraction patterns of quenched products at different distance x from the top the copper cone are shown in Fig. 4. The transformation of the reactants to the ferromagnetic lead hexaferrite $\text{PbFe}_{12}\text{O}_{19}$ was completed in the postcombustion zone. The combustion temperature attained its maximum value about 3 s after ignition as shown in Fig. 2(a), and the average combustion velocity was about 0.5 mm/s. Thus, we estimate the width of the total preheating and reaction zone ~ 1.5 mm. The XRD pattern shows that the magnetite phase Fe_3O_4 (cubic $Fd\bar{3}m$ space group $a = 8.396$ Å, and $Z = 8$) was mainly present in the combustion front zone at $x = 1.5$ mm. A small amount of the reactant Fe_2O_3 and intermediate phases PbFe_4O_7 and PbO were also present. This suggests that partial iron oxidation and total decomposition of the lead nitrate occur in this zone. The formation of the

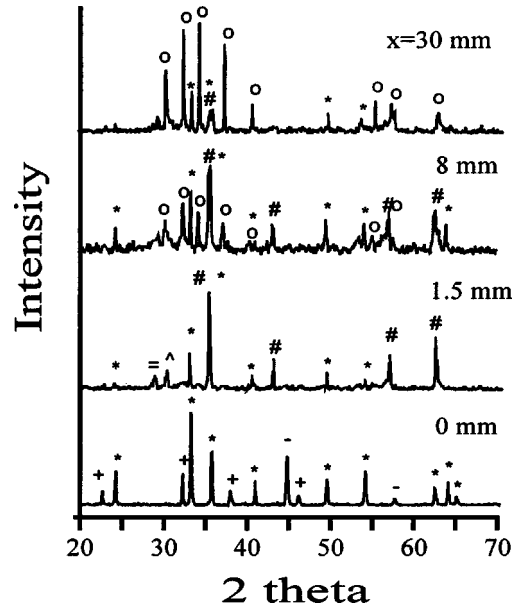
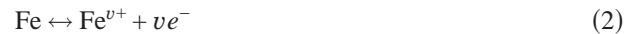


FIG. 4. X-ray powder diffraction plots obtained during combustion synthesis of lead hexaferrite in an air. Patterns detected using the quench front method from locations at a distance x from top of the cone. ($x = 0$ mm) green charge; ($x = 1.5$ mm) preheated and combustion zone; ($x = 8$ and 30 mm) post combustion zone. Key: (+) $\text{Pb}(\text{NO}_3)_2$; (-) Fe ; (*) Fe_2O_3 ; (=) PbO ; (°) PbFe_4O_7 ; (#) Fe_3O_4 ; (○) $\text{PbFe}_{12}\text{O}_{19}$.

hexagonal phase $\text{PbFe}_{12}\text{O}_{19}$ (with lattice parameter $a = 5.872$ Å and $b = 23.125$ Å) began in the post combustion zone at a distance of about 8.0 mm behind the maximum temperature location but before the Curie temperature (450 °C) was reached. The conversion of the reactants to ferromagnetic phase $\text{PbFe}_{12}\text{O}_{19}$ was maximal when the temperature reached the Curie point at the postcombustion zone. These data agree with previous reports of phase transformation during the combustion synthesis of lead ferrites where, instead of lead nitrite, the initial reactant was either PbO or PbO_2 .^{11,12}

A transient electric field up to 2.5 V/cm was generated during the initial stage of the combustion of lead ferrite, before the maximum combustion temperature was attained and when the reaction product was mainly magnetite Fe_3O_4 . This suggests that the electrical field formed while the iron was partially oxidized. The magnetite has n -type electrical conductivity and is a ferrimagnet below 578 °C.^{13,14} Using the combustion model for products which have n -type conductivity,¹⁵ the high-temperature reversible iron oxidation

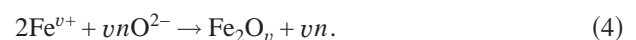


occurs on the iron-oxide interface (a thin exterior oxide layer usually exists on metal particles stored in air).

Two reversible reactions occur on the particle surface: the adsorption of oxygen and its reduction to active anions



and a reaction between the oxygen anions and the metal cations



The total number of surface sites n_t is

$$n_t = n + nO^{2-}, \quad (5)$$

where n is the number of adsorption free sites and nO^{2-} is the number of sites on which oxygen absorbed; v is stoichiometric coefficient. Simultaneously, electron-hole pairs are generated via thermal ionization $e^- + h^+ \leftrightarrow nil$.

At temperatures below 520 °C [the temperature at which the electric signal appeared, Fig. 2(a)] the particles are heated by the approaching temperature front. During this initial period both positive and negative charge carriers are produced on the particles surface. The total concentration of the surface positive and negative charges is very small due to the low combustion temperature. A very small potential difference exists between the surface and the interior of the particle. As the particle heats up, the intrinsic reaction rate and the concentrations of the moving charge carriers increase rapidly and the slow rate of the metal ion diffusion becomes the rate controlling step and the reaction proceeds by the shell progressive mechanism. The different diffusion rate of charge carriers across the growing oxide shell creates an electric double layer. The electrical voltage, its polarity, and amplitude depend on the different charge carrier diffusion velocities. Further interactions in the postcombustion region between Pb^{2+} and iron oxides form lead ferrite but no electric field.

Spontaneous magnetization occurred in the postcombustion zone after the temperature decreased below the Curie temperature and the products were mainly ferromagnetic phases magnetite and lead hexaferrite. We used IR images to follow the temperature during long magnetization process. Several characteristic video pictures at different stages of the reaction are presented in Fig. 5. They show that the temperature of the whole sample was below the Curie temperature about 160 s after ignition. The magnetization curve [Fig. 2(b)] had an inflection point at about that time. We conjecture that the spontaneous magnetization was caused by the orientation of magnetic dipole moments by intrinsic electric fields, which were generated by the differential diffusion of charge carriers through the product layer and by transient magnetic fields during combustion. The magnetic domains orient themselves along the residual field of the bulk material during the long cooling process. Magnetic domains oriented along the applied residual field grow at the expense of domains with random orientation, which shrink. Further magnetic saturation may result from chemisorption, as the adsorption of oxygen molecules on the boundary of a ferromagnetic phase can change the magnetization of the solid.¹⁶ Enhanced dipole moments in intermediate products may be due to the large ionic moments of Fe^{2+} and Fe^{3+} . If the adsorption process involves appreciable electronic interaction and the ratio of surface to volume in the adsorbent is large, then the fractional change of magnetization becomes substantial. We conclude that the spontaneous magnetization rate and the absolute magnetic field value depend on the cooling temperature and ferromagnetic phase formation.

IV. CONCLUSIONS

Transient electric field intensities of up to 2.5 V/cm and current densities of about 5 A/cm² formed during the initial

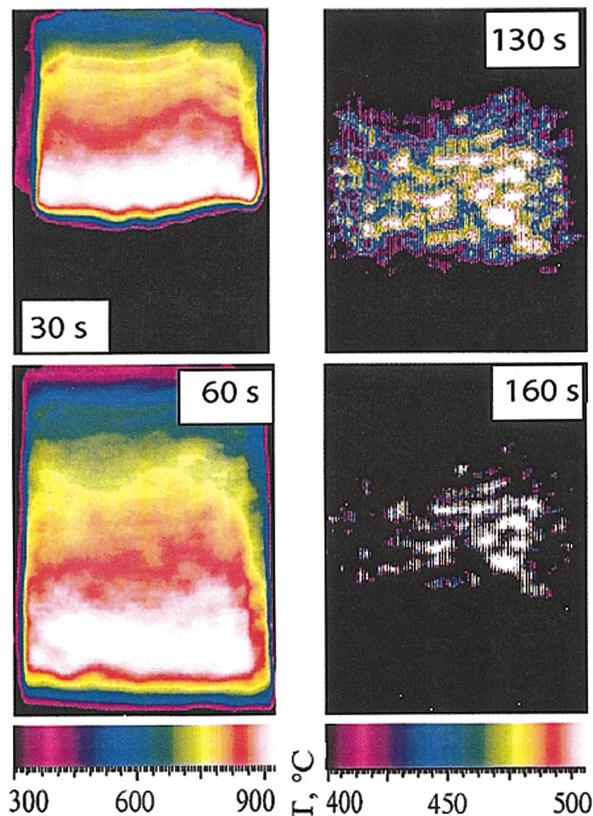


FIG. 5. (Color) The thermo image of a cylindrical sample of lead ferrite measured as a function of time is by IR video camera during the combustion synthesis. Combustion front propagated from top to bottom.

stage of combustion synthesis of lead ferrite, before the maximum combustion temperature was reached. This occurred before the iron oxidation was complete and reaction product mainly consisted of magnetite Fe_3O_4 . The RMF up to 4 μT was associated with spontaneous magnetization in the postcombustion zone in which the conversion of the reactants to ferromagnetic phase $PbFe_{12}O_{19}$ was completed. The characteristic RMF saturation time of about 250 s was much longer than the duration of the electrical signal, 1–2 s. The RMF saturation may be created by three different mechanisms: (i) orientation of magnetic dipole moments by internal electrical field force, (ii) dipole self-orientation along existing residual field of the bulk material during the cooling, and (iii) via chemisorption of O_2 molecules on the ferromagnetic surface. The maximum longitudinal magnetic field component B_l was at the top of the cylindrical sample with the south pole being the ignition location. An almost linear increase of the RMF as a function of sample diameter was probably due to a nonuniform electrical current density in the cross section of the porous medium during the combustion.

ACKNOWLEDGMENTS

The author wish to acknowledge the financial support of this research by the NSF, the Materials Research Science and Engineering Center at the University of Houston, the Robert

A. Welch Foundation (E-1221), the Texas Center for Superconductivity and Advanced Materials, and the Institute for Space Systems Operations.

¹U. Anselmi-Tamburini, Z. A. Munir, J. Appl. Phys. **66**, 5039 (1989).

²A. G. Merzhanov, E. N. Rumanov, Rev. Mod. Phys. **71**, 1173 (1999).

³A. Varma, A. S. Rogachev, A. S. Mukasyan, and S. Hwang, Adv. Chem. Eng. **24**, 79 (1998).

⁴A. G. Merzhanov, S. O. Mkrtchyan, M. D. Nersesyan, P. B. Avakyan, and K. S. Martirosyan, Doklady Akademii Nauk Republic of Armenia **93**, 81 (1992).

⁵M. D. Nersesyan, J. R. Claycomb, Q. Ming, J. H. Miller, J. T. Richardson, and D. Luss, Appl. Phys. Lett. **75**, 1170 (1999).

⁶M. D. Nersesyan, J. T. Ritchie, I. A. Filimonov, J. T. Richardson, and D. Luss, J. Electrochem. Soc. **149**, 11 (2002).

⁷K. S. Martirosyan, I. A. Filimonov, M. D. Nersesyan, and D. Luss, J. Electrochem. Soc. **150**, J9 (2003).

⁸K. S. Martirosyan, I. A. Filimonov, and D. Luss, AIChE J. **50**, 241 (2004).

⁹M. D. Nersesyan, D. Luss, J. R. Claycomb, J. T. Ritchie, and J. H. Miller, Jr., Combust. Sci. Technol. **169**, 89, (2001).

¹⁰K. S. Martirosyan, J. R. Claycomb, G. Gogoshin, R. A. Yarbrough, J. H. Miller, Jr., and D. Luss, J. Appl. Phys. **93**, 9329 (2003).

¹¹K. S. Martirosyan, P. B. Avakyan, and M. D. Nersesyan, Inorg. Mater. **38**, 400 (2002).

¹²K. S. Martirosyan, P. B. Avakyan, and M. D. Nersesyan, Int. J. of Self-propagation High-temperature Synthesis **10**, 193 (2001).

¹³P. Kofstad, *Nonstoichiometry, Diffusion, and Electrical Conductivity in Binary Metal Oxides* (Wiley-Interscience, New York, 1972), p. 382.

¹⁴J. Garcia, G. Subias, M. G. Proietti, H. Renevier, Y. Joly, J. L. Hodeau, J. Blasco, M. C. Sanchez, and J. F. Berar, Phys. Rev. Lett. **85**, 578 (2000).

¹⁵H. Rode, V. Hlavacek, H. J. Viljoen, and J. E. Gatica, Combust. Sci. Technol. **88**, 153 (1992).

¹⁶P. W. Selwood, *Chemisorption and Magnetization* (Academic, New York, 1975), p. 172.